 DOI: 10.1002/masy.201051021

Enhanced Photostability and Red-NIR Photosensitivity of Conjugated Polymer Charge-Transfer Complexes

Anastasiya E. Ozimova,[1] *Vladimir V. Bruevich,*[1] *Thomas Dittrich,*[2] *Dmitry Yu. Paraschuk**[1]

Summary: A promising route to photostable and low-bandgap polymer materials for optoelectronic and photonic applications could be utilization of donor-acceptor ground-state charge-transfer complexes (CTCs) of wide-bandgap conjugated polymers. In this work, we report our results on photostability and photoelectric studies of CTC between an archetypical conjugated polymer MEH-PPV and low-molecular-weight acceptor 2,4,7-trinitrofluorenone (TNF). By using the pump-probe laser photobleaching technique, we show that the photodegradation rate of MEH-PPV:TNF blend films decreases up to four orders of magnitude as compared with pristine MEH-PPV. By using photocurrent and surface photovoltage spectroscopies, we demonstrate that the photoelectric sensitivity of the MEH-PPV:TNF CTC can be deeply extended in the polymer optical gap down to 1 μm. However, the main drawback of the CTC studied is their low charge collection efficiency, and an approach to increasing it is discussed.

Keywords: charge-transfer complexes; conjugated polymers; degradation; low-bandgap materials; solar cells

Introduction

Low-bandgap and photostable conjugated polymer materials are in great demand for photoelectric and photonic applications. A promising route to these materials could be utilization of Mulliken type donor-acceptor ground-state charge-transfer complexes (CTCs) based on conjugated polymers. We found that an archetypical conjugated polymer, poly[2-methoxy-5-(2′-ethyl-hexyloxy)-1,4-phenylene vinylene] (MEH-PPV), can form the CTCs with some low-molecular-weight organic acceptors,[1] e.g., with 2,4,7-trinitrofluorenone (TNF). CTCs of this type have a number of attractive properties for their usage in solar cells and photodetectors.[2] For example, their effective bandgap (Figure 1) can be tuned down to the near-infrared (NIR) by variation of the acceptor electron affinity, and the efficiency of ultrafast charge photogeneration in the CTCs is as high as in polymer-fullerene blends.[3] Moreover, the CTC formation dramatically improves the photooxidation stability of the blend.[4]

In this paper, we report our results on photostability and photoelectric studies of MEH-PPV:TNF CTCs. We study photodegradation of MEH-PPV:TNF blend films by a laser photobleaching method.[5] In its simplest version, a laser beam irradiates the sample, and its optical transmission is recorded during irradiation. The method allows evaluation of the photobleaching rate that is for PPVs assigned to photo-

[1] Faculty of Physics and International Laser Center, M.V. Lomonosov Moscow State University, Leninskie Gory 1, 119991 Moscow, Russia
Fax: +7 (495) 9393113;
E-mail: paras@physics.msu.ru
[2] Helmholtz-Zentrum Berlin für Materialien und Energie, Heterogene Materialsysteme, Glienicker Str. 100, 14109 Berlin, Germany

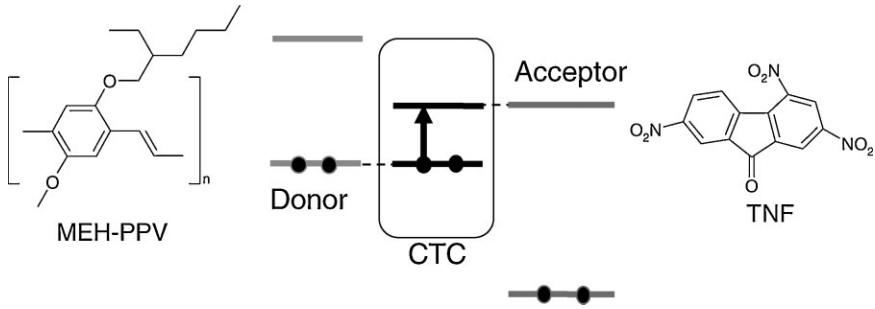

Figure 1.
Schematic of frontier molecular orbitals of donor (MEH-PPV), acceptor (TNF), and CTC.

oxidation of the chromophores.[6] Earlier, the laser photobleaching method was used for photostability study of a substituted PPV.[7] We show that the photobleaching rate of MEH-PPV:TNF blends decreases up to four orders of magnitude as compared with pristine MEH-PPV. Another promising feature of conjugated polymer CTCs is their pronounced absorption in the red and NIR spectral ranges[1,8] that could be used as an approach to organic low-bandgap materials for solar cells and photodetectors. In this work, we study the photosensitiviy of the MEH-PPV:TNF CTC by photocurrent and surface photovoltage (SPV) spectroscopies. If the photoelectric measurements on the device structures deliver aggregated information about charge photogeneration, their transport and collection at the electrodes, the SPV techniques can directly probe spatially separated charges without the top electrical contact of the device. The latter is important as the interface at the top electric contact of the device unavoidably contributes to the measured signal that can complicate the extraction of information about spatial separation of photoinduced charges in the material. The SPV technique was initially developed and is commonly applied to study charge separation in inorganic semiconductors[9] but insofar it is much less used to probe charge separation in materials based on semiconducting polymers. Our SPV data indicate that the photosensitive range of MEH-PPV:TNF tends to the NIR down to 1 μm.

Experimental Part

MEH-PPV (Sigma-Aldrich, $M_n = 70{,}0000$–$100{,}000$) and TNF were separately dissolved in chlorobenzene at concentration 1–5 g/l. Blends were prepared by mixing the polymer and acceptor solutions with appropriate molar ratio. Films were prepared on glass substrates by spin-casting at 1000 rpm. Absorption spectra of the films were measured by using a monochromator equipped with a tungsten-halogen lamp and a silicon photodetector.

To study the photooxidation stability of MEH-PPV:TNF films under ambient conditions, we use the pump-probe laser photobleaching technique described elsewhere.[9] Briefly, a pump laser beam at 514 nm irradiates the film, and a probe laser beam at 532 nm probes the film transmission. The intensity of the pump beam was about 3 W/cm^2. The probe beam transmission is recorded as a function of irradiation time by using a silicon photodetector and processed by a lock-in amplifier to improve the signal-to-noise ratio. Then, the photobleaching rate is calculated from the probe transmission kinetics according to Refs.[5,9].

To probe spatially separated photoinduced charges, we use SPV spectroscopy technique described elsewhere.[10] In brief, the light dispersed by a quartz-prism monochromator equipped with a tungsten-halogen lamp excites a drop-cast film under study deposited on an ITO-covered glass substrate. The SPV is measured by

using lock-in technique at a chopping frequency of 8 Hz in the capacitor arrangement with a thin mica layer used as a spacer between the semi-transparent Cr electrode and the film surface. Alternatively, the sample can be photoexcited through the ITO-electrode.

For the photocurrent measurements, sandwich-type samples were prepared on the ITO-covered glass substrates. A PEDOT:PSS layer was spin-cast onto the ITO-side. After that, an active layer was spin-cast at 1000–1500 rpm on the PEDOT:PSS layer from MEH-PPV:TNF solution. The active layer absorbed less than 50% of the incident light (the thickness did not exceed 50 nm) so that the internal filtering effect can be neglected. Then Al contacts were thermally deposited onto the active layer. Photodiodes were illuminated through the substrate by a spectrally-dispersed tungsten-halogen lamp, and the preamplified photocurrent was measured by a lock-in amplifier at a 75 Hz modulation frequency.

Results and Discussion

Photobleaching Data

Figure 2 compares evolution of the absorption spectra of pristine MEH-PPV and 1:1 MEH-PPV:TNF films under laser irradiation. As Figure 2a shows, during irradiation, the pristine MEH-PPV photobleaches: its absorption decreases, and its spectrum shifts to the blue spectral range. This photobleaching effect in PPVs is well documented and assigned to photooxidation of the conjugated chains.[6,11] On the contrary, as Figure 2b shows, photobleaching in the 1:1 MEH-PPV:TNF blend is completely suppressed indicating dramatic enhancement in the photooxidation stability of MEH-PPV:TNF blends.

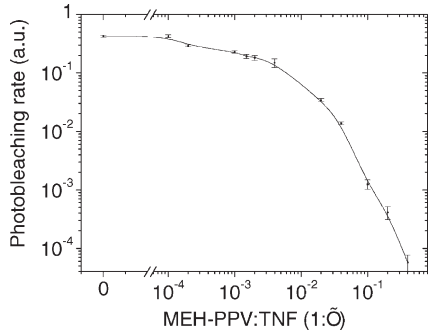

Figure 3.
Photobleaching rate of MEH-PPV:TNF films vs TNF content. The line is a guide to the eye.

Figure 3 shows the photobleaching rate of MEH-PPV in MEH-PPV:TNF blends as a function of TNF content measured by the pump-probe laser photobleaching technique. The photobleaching rate starts to decrease at TNF concentration as low as 10^{-4} and then monotonically drops. For the TNF content more than 0.01, the photobleaching rate is drastically decreased, and for TNF:MEH-PPV ratio

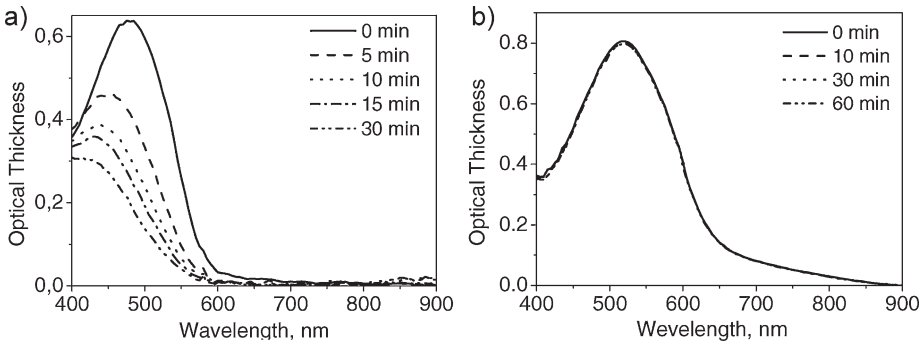

Figure 2.
Absorption spectra of pristine MEH-PPV (a) and blend 1:1 MEH-PPV:TNF (b) spin-cast films after laser irradiation at 532 nm with intensity 110 mW/cm^2. Accumulated irradiation time is indicated in the figure.

higher than 0.2 the photobleaching rate is beyond the experimental resolution. As Figure 3 shows, the overall drop in the photobleaching rate for 1:0.4 MEH-PPV:TNF blend is about four orders of magnitude as compared to pristine MEH-PPV. The observed enhancement in photostability of MEH-PPV in MEH-PPV:TNF blends is in good agreement with the recent photostability data on these blends obtained by FTIR spectroscopy.[4] Therefore, it is natural to assign the observed drop in the photobleaching rate of the blends with decrease in the photooxidation rate of MEH-PPV. The photostability enhancement in MEH-PPV:TNF blends was explained by blocking of formation of triplet excitons at the polymer,[4] which are known to be one of the key precursors for photooxidation of PPVs.[12] This triplet blocking can be due to fast energy transfer from photoexcited MEH-PPV conjugated segments to CTC.[13]

Photocurrent Spectroscopy Data

Figure 4 shows photocurrent action spectra of MEH-PPV:TNF photodiodes for different polymer:acceptor ratios in terms of the external quantum efficiency (EQE), i.e., the probability of an incident photon to generate a pair of charge carriers at the device electrodes. Addition of TNF results in a considerable increase of the EQE in the MEH-PPV optical gap; therefore, the photoexcited CTC generates mobile charges. The photocurrent spectrum for the equimolar donor:acceptor ratio in Figure 4 correlates well with the corresponding absorption spectrum in Figure 2b. This correlation indicates the similar charge generation efficiencies over the entire investigated spectral region that is in accordance with the ultrafast photoinduced absorption spectroscopy data.[14] However, the EQE is quite low (no much than 0.1%) as compared to well-studied MEH-PPV:fullerene blends.

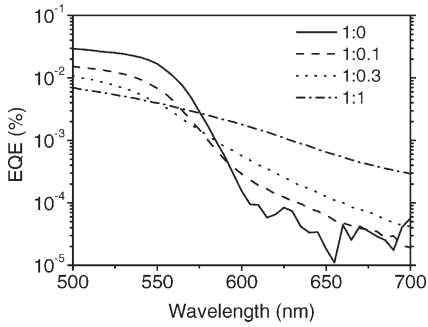

Figure 4.
Photocurrent action spectra of MEH-PPV:TNF photodiodes for different donor:acceptor molar ratios.

From the ultrafast photoinduced absorption spectroscopy data,[3] such low EQEs are attributed to the efficient charge recombination in the blends with CTCs but *not* to inefficient photon-to-charge conversion. However, the geminate recombination alone seems to be not sufficient to account for the observed a few orders of magnitude difference in the EQEs of the blends with CTCs and polymer:fullerene blends as, according the picosecond photoinduced absorption data,[3] the concentration of long-lived charges differs by a factor of ~10 in the CTC and MEH-PPV:fulerene blends. We assign the observed low EQEs also to the low charge collection efficiency resulting from low charge mobilities in blends with CTC. This assignment is supported by previous studies on poly-n-vinylcarbazole:TNF CTC[15] where typical electron and hole mobilities below 10^{-6} cm^2/Vs were observed in the blends.

One might expect that increasing the acceptor content in the CTC films could increase the charge collection efficiency as it does in the case of the polymer:fullerene blends due to formation of the efficient charge collection network resulting from the donor:acceptor phase separation. As was shown earlier,[16] formation of the separated acceptor phase in MEH-PPV:TNF blends starts at acceptor:polymer ratio higher than 0.3:1. Indeed, the EQE in the range 600–700 nm is considerably higher in the 1:1 blend than in the 1:0.3 blend (Figure 4) that can be attributed to the enhanced charge collection due to formation of the acceptor phase. However, the much higher EQE within the region of MEH-PPV strong absorption, i.e., in the

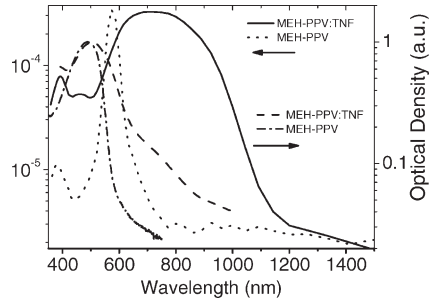

Figure 5.
SPV spectra of 1:0.6 MEH-PPV:TNF (solid) and pristine MEH-PPV (dotted) drop-cast films and their absorption spectra (dashed and dash-dotted curves, respectively). The SPV spectra are shown without correction to the incident spectrum.

spectral range 500–580 nm, tends to decrease with addition of TNF (Figure 4). Moreover, the maximum EQE in MEH-PPV:TNF blends is even lower than that in the pristine MEH-PPV device. Possibly, this results from the inefficient charge collection network in MEH-PPV:TNF blends that can collect only very limited amount of chargers.

Surface Photovoltage Spectroscopy Data

Figure 5 compares SPV spectra of pristine MEH-PPV and MEH-PPV:TNF films; their optical absorption spectra are also shown for comparison. The SPV spectrum of the pristine MEH-PPV film nearly follows the edge of its absorption spectrum indicating that the absorbed photons generate spatially separated charges. However, at shorter wavelengths (<580 nm), the SPV signal in the pristine MEH-PPV strongly decreases, whereas the optical absorption increases (Figure 5). This antibatic behavior of the photovoltage and absorption spectra was far less pronounced in thinner films. In addition, for illumination of the sample from the other side (through the glass substrate), the SPV spectrum was symbatic with the absorption spectrum. These observations indicate that spatial charge separation in pristine MEH-PPV occurs mainly at the ITO/film interface. The antibatic behavior of the SPV and absorption spectra can be assigned mainly to the internal filter effect, i.e., to the effect of an optically thick film absorbing the photons before they reach the ITO/film interface.

In the 1:0.6 MEH-PPV:TNF film, the SPV spectrum shows the onset at 1.1 μm (Figure 5). It is reasonble to assign the SPV signal in the MEH-PPV optical gap to the CTC absorption band. Accordingly, the photoexcited CTC generates spatially separated charges that is in agreement with the above photocurrent spectroscopy data. The onset of the SPV spectrum we assign to the CTC absorption edge, which is difficult to identify in the optical absorption spectra in Figure 1b. The SPV spectrum of the MEH-PPV:TNF film exhibits a broad band in the range 600–900 nm as compared with the narrow band at 580 nm for the pristine MEH-PPV (Figure 5). This difference in width can be partially assigned to a broad and less intensive CTC absorption spectrum that results in the internal filter effect only for wavelengths shorter than 650 nm. As follows from the SPV spectra in the range 350–600 nm (Figure 5), the internal filter effect is less pronounced in the blend than in the pristine MEH-PPV despite both films are optically thick. Moreover, we have observed that the shape of the SPV spectra does not evolve monotonically with addition of TNF. These observations indicate that the mechanism of charge generation in MEH-PPV:TNF blends is different from that of the pristine polymer. Presumably, in the latter, the charges are separated mainly at the polymer/ITO interface, whereas, in the former, the charges are separated in the bulk.

Conclusion

Our laser photobleaching studies on MEH-PPV:TNF blend films indicate that these blends can be highly photostable against photooxidation under ambient conditions. Our photobleaching data are in good agreement with the recent results on photooxidation stability of MEH-

PPV:TNF blends obtained with the use of FTIR technique.[4] As follows from the photocurrent and SPV spectroscopy data, the photoelectric sensitivity of the MEH-PPV:TNF CTC can be deeply extended in the polymer optical gap down to 1 μm. Moreover, one may expect that the photosensitivity edge could be shifted further in the NIR by using organic acceptors with higher electron affinity than that of TNF. Indeed, the Mulliken model suggests that the optical gap of the CTC (Figure 1) is scaled with the difference between the acceptor LUMO and donor HOMO energies. However, the crucial drawbacks in the studied CTCs are efficient geminate recombination of photogenerated charges[3] and their poor collection at the electrodes. These drawbacks can be partially attributed to low electron mobility of TNF. In fact, pristine TNF films show the electron mobility in the range 10^{-5} cm^2/Vs,[15] which is too low for efficient charge collection in the bulk heterojunctions. Possibly, using the CTC-acceptors with high electron mobility could considerably increase the charge collection efficiency in blends with CTCs. Furthermore, to enhance generation of long-lived charges and their collection, one could use CTC doped with fullerene, i.e., appropriate ternary blends. As has been recently shown, a consecutive photo-induced electron transfer from the polymer to the CTC-acceptor in the first step and then, in the second step, to the fullerene is realized in the ternary blend.[17] This approach allows combining the benefits of conjugated polymer CTCs such as strong absorption in the polymer optical gap and enhanced photooxidation stability with the advantages of fullerenes such as efficient agents in generation of charge-separated states and high charge mobility. Thus, conjugated polymer CTCs can be a promising route for photostable and low-bandgap materials for optoelectronic and photonic applications if the efficient ways for suppressing geminate recombination of charges in the CTCs and improving their collection are found.

Acknowledgements: This work is partially supported by the Russian Foundation for Basic Research (project 08-02-12170-ofi). We thank A.A. Gromchenko for her help in device preparation and D.S. Martyanov for his contribution at the early stage of this work and discussions.

[1] A. A. Bakulin, S. G. Elizarov, A. N. Khodarev, D. S. Martyanov, I. V. Golovnin, D. Y. Paraschuk, M. M. Triebel, I. V. Tolstov, E. L. Frankevich, S. A. Arnautov, E. M. Nechvolodova, *Synth. Met.* **2004**, *147*, 221.
[2] A. A. Bakulin, M. S. Pshenichnikov, P. H. M. van Loosdrecht, I. V. Golovnin, D. Y. Paraschuk, in: *Physics of nanostructured solar cells*, V. Badescu, M. Paulescu, Eds., Nova Science Publishers, **2009**.
[3] A. A. Bakulin, D. S. Martyanov, D. Y. Paraschuk, M. S. Pshenichnikov, P. H. M. van Loosdrecht, *J. Phys. Chem. B* **2008**, *112*, 13730.
[4] I. V. Golovnin, A. A. Bakulin, S. A. Zapunidy, E. M. Nechvolodova, D. Y. Paraschuk, *Appl. Phys. Lett.* **2008**, *92*, 243311.
[5] K. K. Boyarsky, A. Y. Vorobev, V. I. Zemsky, Y. L. Kolesnikov, I. K. Meshkovsky, *Opt Spektrosk.* **1988**, *65*, 909.
[6] L. J. Rothberg, M. Yan, F. Papadimitrakopoulos, M. E. Galvin, E. W. Kwock, T. M. Miller, *Synth. Met.* **1996**, *80*, 41.
[7] E. G. J. Staring, A. J. M. Berntsen, S. T. R. Romme, G. Rikken, P. Urbach, *Philos. Trans. R. Soc. London, Ser. A* **1997**, *355*, 695.
[8] D. Y. Paraschuk, S. G. Elizarov, A. N. Khodarev, A. N. Shchegolikhin, S. A. Arnautov, E. M. Nechvolodova, *JETP Lett.* **2005**, *81*, 467.
[9] A. E. Ozimova, V. V. Bruevich, D. Y. Paraschuk, in preparation.
[10] V. Duzhko, V. Y. Timoshenko, F. Koch, T. Dittrich, *Phys. Rev. B* **2001**, *64*, 075204.
[11] B. H. Cumpston, K. F. Jensen, *Synth. Met.* **1995**, *73*, 195.
[12] L. C. Ma, X. S. Wang, B. J. Wang, J. R. Chen, J. H. Wang, K. Huang, B. W. Zhang, Y. Cao, Z. H. Han, S. P. Qian, S. D. Yao, *Chem. Phys.* **2002**, *285*, 85.
[13] S. A. Zapunidi, Y. V. Krylova, D. Y. Paraschuk, *Phys. Rev. B* **2009**, *79*, 205208.
[14] A. A. Bakulin, D. Martyanov, D. Y. Paraschuk, P. H. M. van Loosdrecht, M. S. Pshenichnikov, *Chem. Phys. Lett.* submittted.
[15] D. Gill, *J. Appl. Phys.* **1972**, *43*, 5034.
[16] S. G. Elizarov, A. E. Ozimova, D. Y. Paraschuk, S. A. Arnautov, E. M. Nechvolodova, *Proc. SPIE* **2006**, *6257*, 293.
[17] A. A. Bakulin, S. A. Zapunidy, M. S. Pshenichnikov, P. H. M. van Loosdrecht, D. Y. Paraschuk, *Phys. Chem. Chem. Phys.* **2009**, *33*, 7324.

